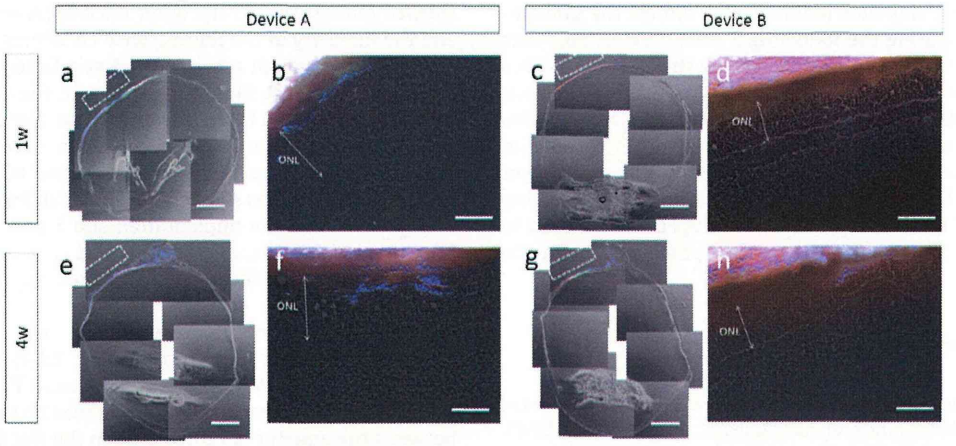

Fig. 6. (a–h) The distribution of FL (green), Rho (red) and DAPI (blue) in the retina and sclera around the implantation site 1 week (a–d) and 4 weeks (e–h) after implantation (square dots: device implantation site). Two types of devices, device A (F60/R40/D60) and B (F60/R60/D40), were used. Device A shows faster DAPI release than Rho and device B shows faster Rho release than DAPI. Magnified images (b, d, f, h) show that fluorescents reached the outer nuclear layer (ONL, double-headed allows). Scale bars, 1 mm (a, c, e, g) and 100 μm (b, d, f, h).

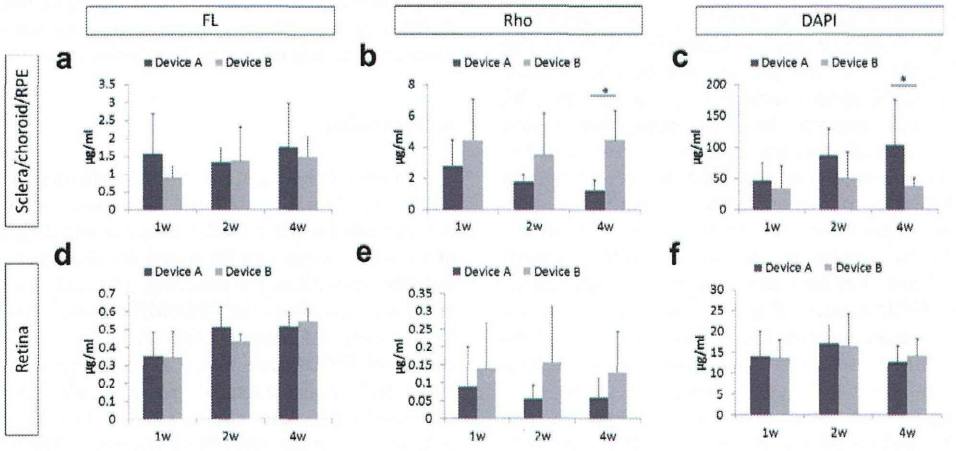

Fig. 7. The amounts of FL, Rho and DAPI in the sclera/choroid/RPE (a–c) and retinal fractions (d–f) during 4 weeks' implantation. Values are mean ± SD. $^{*}p < 0.05$ (unpaired *t*-test for normally distributed isolated pairs).

conditions (Supplementary Fig. S.2), indicating that the permeability may be influenced by the physical characteristics of the substance, such as lipophilicity, water solubility and acid–base character; FL and Rho-B are weak carboxylic acids, while DAPI is a base [33]. Therefore, we need to consider the physical characteristics of the substances and their interactions when determining the optimum PEGDM/TEGDM system for the intended drug release.

The device materials, PEGDM and TEGDM, are bio-inert and can be easily molded into different substrate shapes by UV curing [34,35]. We used a microfabrication technique because the shape and volume of the reservoir can be easily modified by an AutoCAD design. We have previously reported a reservoir-based protein-drug-release device sealed with a PEGDM cover including collagen microparticles, which served as permeation porogen for macromolecules [36]. We found that low-molecular-weight molecules can easily pass through polymerized PEGDM membrane, whereas polymerized TEGDM is impermeable to them (Fig. 2). Therefore, we newly developed a controlled release system for low-molecular-weight drugs using a PEGDM/TEGDM mixture. Some monomers of unpolymerized PEGDM and TEGDM and photoinitiator were found to elute from the device, but the amount of elution (the highest amount is 504 ng ml^{-1}) was significantly less than cytotoxically active levels (more than 391 μg ml^{-1}), and no more monomers and photoinitiator eluted after incubation in PBS for 15 days (Supplementary Fig. S.4). The PEGDM/TEGDM polymer shows almost no biodegradation 19 months after implantation on the rabbit sclera (Supplementary Fig. S.5). Additionally, the long-term implantation of the device over 4 weeks did not affect retinal function assessed by electroretinograms (Supplementary Fig. S.6). Thus, the device would appear to be stable and biocompatible for at least 1 year, and can be used to safely administer drugs by the transscleral approach without disturbing intraocular tissues.

Fluorescents were used for the analysis of drug transport into the eye from the device. Although fluorescence was observable in the ocular tissues during 4 weeks' implantation and distributed locally around the implantation site, the fluorescein concentration in the retina seemed to be almost the same in spite of the difference in the release profiles of the devices (Figs. 4f and 7e and f). This may be due to the blood–retinal barrier restricting drug transport through the RPE to the retina. Pitkanen reported that the permeability through the RPE depended on the lipophilicity and molecular weight of drugs [37]. Additionally, transporters in the RPE probably have a greater role in ocular pharmacokinetics [38]. In

fact, we observed FL accumulation around the RPE (Fig. 4d), indicating that the drug transport was restricted here. This may be one of the reasons for the constant amount of fluorescents in the retina. Additionally, this behavior might be due to the availability of fluorescents at the retina, because transport and penetration through the sclera, choroid and RPE may vary between molecules [37]. The clearance rate by blood vessels may also be different for hydrophobic and hydrophilic molecules [15]. Our device has a low-molecular-weight-impermeable reservoir that can release drugs unidirectionally to the sclera, making it less susceptible to drug elimination by conjunctival lymphatic/blood vessel clearance, so the choroid may be the primary route of clearance. Further study is needed to elucidate the factors influencing drug availability to the retina. Given that the distribution of fluorescents was concentrated at the RPE and adjacent regions, our device may be effective, especially for lesions in the vicinity of the RPE.

One of the limitations of this study is the lack of a study proving retinal neuroprotective effects of our device using clinical drugs. Previous reports show potent effective drugs, such as edaravone [39], geranylgeranylaceton [40] and unoprostone [41] against retinal degeneration in animals, whereas these drugs are administered via systemic route, topical eye drop or intravitreal injection. We are planning to perform an animal study using the clinical drugs to investigate the efficacy of our controlled transscleral multi-drug delivery system on retinal neuroprotection.

5. Conclusion

A polymeric system which can administer multiple compounds with distinct kinetics to the posterior segment of the eye was manufactured. The release of multiple compounds can be tuned by changing their formulations as well as the device covering. Furthermore, our system can be used to safely administer drugs by the transscleral approach without disturbing intraocular tissues. Strict local delivery of the drugs through our device may facilitate the administration of the drugs that would not be suitable for systemic use due to side-effects. Additionally, prolonged sustained drug release using our device would be suitable for the treatment of chronic retinal diseases. Thus, our polymeric system provides prolonged action and less invasive intraocular administration, and is expected to provide new tools for the treatment of posterior eye diseases with new therapeutic modalities.

Competing financial interests

The authors declare no conflict of interest.

Acknowledgements

This study was supported by Grant-in-Aid for Young Scientists (A) from the Ministry of Education, Culture, Sports, Science, and Technology 23680054 (N.N.), Health Labour Sciences Research Grant from the Ministry of Health Labour and Welfare H23-iryokiki-wakate-003 (N.N.), H23-kankaku-ippan-004 (T.A. and N.N.), H24-nanchitoh-ippan-067 (T.A. and N.N.), the Takeda Science Foundation (N.N.), the Tohoku University Exploratory Research Program for Young Scientists (N.N.) and Gonryo Medical Foundation (N.N.). We thank T. Kawashima, N. Kumasaka, T. Yamada and S. Ito for help with device molds preparation.

Appendix A. Supplementary data

Supplementary data associated with this article can be found, in the online version, at http://dx.doi.org/10.1016/j.actbio.2013.11.004.

References

[1] Resnikoff S, Pascolini D, Etya'ale D, Kocur I, Pararajasegaram R, Pokharel GP, et al. Global data on visual impairment in the year 2002. Bull World Health Organ 2004;82:844–51.
[2] Gragoudas ES, Adamis AP, Cunningham Jr ET, Feinsod M, Guyer DR. Pegaptanib for neovascular age-related macular degeneration. N Engl J Med 2004;351:2805–16.
[3] Kim M, Yoon BJ. Adaptive reference update (ARU) algorithm. A stochastic search algorithm for efficient optimization of multi-drug cocktails. BMC Genomics 2012;13(Suppl 6):S12.
[4] Calkins DJ. Critical pathogenic events underlying progression of neurodegeneration in glaucoma. Prog Retin Eye Res 2012;31:702–19.
[5] Fu QL, Li X, Yip HK, Shao Z, Wu W, Mi S, et al. Combined effect of brain-derived neurotrophic factor and LINGO-1 fusion protein on long-term survival of retinal ganglion cells in chronic glaucoma. Neuroscience 2009;162:375–82.
[6] Shin DH, Feldman RM, Sheu WP. Efficacy and safety of the fixed combinations latanoprost/timolol versus dorzolamide/timolol in patients with elevated intraocular pressure. Ophthalmology 2004;111:276–82.
[7] Spaide RF. Rationale for combination therapy in age-related macular degeneration. Retina 2009;29:S5–7.
[8] He S, Xia T, Wang H, Wei L, Luo X, Li X. Multiple release of polyplexes of plasmids VEGF and bFGF from electrospun fibrous scaffolds towards regeneration of mature blood vessels. Acta Biomater 2012;8:2659–69.
[9] Campochiaro PA. Potential applications for RNAi to probe pathogenesis and develop new treatments for ocular disorders. Gene Ther 2006;13:559–62.
[10] Frasson M, Picaud S, Leveillard T, Simonutti M, Mohand-Said S, Dreyfus H, et al. Glial cell line-derived neurotrophic factor induces histologic and functional protection of rod photoreceptors in the rd/rd mouse. Invest Ophthalmol Vis Sci 1999;40:2724–34.
[11] Rosenfeld PJ, Brown DM, Heier JS, Boyer DS, Kaiser PK, Chung CY, et al. Ranibizumab for neovascular age-related macular degeneration. N Engl J Med 2006;355:1419–31.
[12] Hughes PM, Olejnik O, Chang-Lin JE, Wilson CG. Topical and systemic drug delivery to the posterior segments. Adv Drug Deliv Rev 2005;57:2010–32.
[13] Del Amo EM, Urtti A. Current and future ophthalmic drug delivery systems. A shift to the posterior segment. Drug Discov Today 2008;13:135–43.
[14] Geroski DH, Edelhauser HF. Transscleral drug delivery for posterior segment disease. Adv Drug Deliv Rev 2001;52:37–48.
[15] Ranta VP, Urtti A. Transscleral drug delivery to the posterior eye: prospects of pharmacokinetic modeling. Adv Drug Deliv Rev 2006;58:1164–81.
[16] Ambati J, Adamis AP. Transscleral drug delivery to the retina and choroid. Prog Retin Eye Res 2002;21:145–51.
[17] Olsen TW, Edelhauser HF, Lim JI, Geroski DH. Human scleral permeability. Effects of age, cryotherapy, transscleral diode laser, and surgical thinning. Invest Ophthalmol Vis Sci 1995;36:1893–903.
[18] Li X, Zhang Z, Li J, Sun S, Weng Y, Chen H. Diclofenac/biodegradable polymer micelles for ocular applications. Nanoscale 2012;4:4667–73.
[19] Patel SR, Berezovsky DE, McCarey BE, Zarnitsyn V, Edelhauser HF, Prausnitz MR. Targeted administration into the suprachoroidal space using a microneedle for drug delivery to the posterior segment of the eye. Invest Ophthalmol Vis Sci 2012;53:4433–41.
[20] Aksungur P, Demirbilek M, Denkbas EB, Vandervoort J, Ludwig A, Unlu N. Development and characterization of Cyclosporine A loaded nanoparticles for ocular drug delivery: cellular toxicity, uptake, and kinetic studies. J Control Release 2011;151:286–94.
[21] Chhablani J, Nieto A, Hou H, Wu EC, Freeman WR, Sailor MJ, et al. Oxidized porous silicon particles covalently grafted with daunorubicin as a sustained intraocular drug delivery system. Invest Ophthalmol Vis Sci 2013;54:1268–79.
[22] Chen CW, Lu DW, Yeh MK, Shiau CY, Chiang CH. Novel RGD-lipid conjugate-modified liposomes for enhancing siRNA delivery in human retinal pigment epithelial cells. Int J Nanomedicine 2011;6:2567–80.
[23] Kaiser JM, Imai H, Haakenson JK, Brucklacher RM, Fox TE, Shanmugavelandy SS, et al. Nanoliposomal minocycline for ocular drug delivery. Nanomedicine 2013;9:130–40.
[24] Li X, Zhang Z, Chen H. Development and evaluation of fast forming nanocomposite hydrogel for ocular delivery of diclofenac. Int J Pharm 2013;448:96–100.
[25] Wang CH, Hwang YS, Chiang PR, Shen CR, Hong WH, Hsiue GH. Extended release of bevacizumab by thermosensitive biodegradable and biocompatible hydrogel. Biomacromolecules 2012;13:40–8.
[26] Kunou N, Ogura Y, Yasukawa T, Kimura H, Miyamoto H, Honda Y, et al. Long-term sustained release of ganciclovir from biodegradable scleral implant for the treatment of cytomegalovirus retinitis. J Control Release 2000;68:263–71.
[27] Zhang H, Zhao C, Cao H, Wang G, Song L, Niu G, et al. Hyperbranched poly(amine-ester) based hydrogels for controlled multi-drug release in combination chemotherapy. Biomaterials 2010;31:5445–54.
[28] Shin HC, Alani AW, Rao DA, Rockich NC, Kwon GS. Multi-drug loaded polymeric micelles for simultaneous delivery of poorly soluble anticancer drugs. J Control Release 2009;140:294–300.
[29] Richardson TP, Peters MC, Ennett AB, Mooney DJ. Polymeric system for dual growth factor delivery. Nat Biotechnol 2001;19:1029–34.
[30] Lammers T, Subr V, Ulbrich K, Peschke P, Huber PE, Hennink WE, et al. Simultaneous delivery of doxorubicin and gemcitabine to tumors in vivo using prototypic polymeric drug carriers. Biomaterials 2009;30:3466–75.

[31] Elia R, Fuegy PW, VanDelden A, Firpo MA, Prestwich GD, Peattie RA. Stimulation of in vivo angiogenesis by in situ crosslinked, dual growth factor-loaded, glycosaminoglycan hydrogels. Biomaterials 2010;31:4630–8.
[32] Wang Y, Wang B, Qiao W, Yin T. A novel controlled release drug delivery system for multiple drugs based on electrospun nanofibers containing nanoparticles. J Pharm Sci 2010;99:4805–11.
[33] Dickens SH, Flaim GM, Floyd CJ. Effects of adhesive, base and diluent monomers on water sorption and conversion of experimental resins. Dent Mater 2010;26:675–81.
[34] Benoit DS, Durney AR, Anseth KS. Manipulations in hydrogel degradation behavior enhance osteoblast function and mineralized tissue formation. Tissue Eng 2006;12:1663–73.
[35] Kalachandra S. Influence of fillers on the water sorption of composites. Dent Mater 1989;5:283–8.
[36] Kawashima T, Nagai N, Kaji H, Kumasaka N, Onami H, Ishikawa Y, et al. A scalable controlled-release device for transscleral drug delivery to the retina. Biomaterials 2011;32:1950–6.
[37] Pitkanen L, Ranta VP, Moilanen H, Urtti A. Permeability of retinal pigment epithelium: effects of permeant molecular weight and lipophilicity. Invest Ophthalmol Vis Sci 2005;46:641–6.
[38] Mannermaa E, Vellonen KS, Urtti A. Drug transport in corneal epithelium and blood-retina barrier: emerging role of transporters in ocular pharmacokinetics. Adv Drug Deliv Rev 2006;58:1136–63.
[39] Imai S, Inokuchi Y, Nakamura S, Tsuruma K, Shimazawa M, Hara H. Systemic administration of a free radical scavenger, edaravone, protects against light-induced photoreceptor degeneration in the mouse retina. Eur J Pharmacol 2010;642:77–85.
[40] Tanito M, Kwon YW, Kondo N, Bai J, Masutani H, Nakamura H, et al. Cytoprotective effects of geranylgeranylacetone against retinal photooxidative damage. J Neurosci 2005;25:2396–404.
[41] Tsuruma K, Tanaka Y, Shimazawa M, Mashima Y, Hara H. Unoprostone reduces oxidative stress- and light-induced retinal cell death, and phagocytotic dysfunction, by activating BK channels. Mol Vis 2011;17:3556–65.

Combined 25-Gauge Microincision Vitrectomy and Toric Intraocular Lens Implantation With Posterior Capsulotomy

Hiroshi Kunikata, MD, PhD; Naoko Aizawa, MD; Yasuhiko Meguro, MD; Toshiaki Abe, MD, PhD; Toru Nakazawa, MD, PhD

PURPOSE: To evaluate the efficacy of combined 25-gauge microincision vitrectomy surgery (MIVS) and toric intraocular lens (IOL) implantation with posterior capsulotomy.

METHODS: Noncomparative, interventional case series performed at a single center. Twelve patients with vitreoretinal disease and cataracts, with pre-existing regular corneal astigmatism greater than 1 diopter, underwent 25-gauge MIVS and toric IOL implantation with posterior capsulotomy.

RESULTS: The toric IOL was successfully implanted in each case. At 6 months postoperatively, mean axis rotation was 5.7° ± 3.1°. At 1 month postoperatively, mean uncorrected and best corrected visual acuity improved; the improvement was maintained after 6 months. The absolute residual refractive cylinder was significantly lower postoperatively than the pre-existing regular corneal cylinder (P = .003). There were no surgical complications except a temporary posterior irissynechia in one case.

CONCLUSIONS: Combined 25-gauge MIVS and toric IOL implantation with posterior capsulotomy is a practical and safe method to treat vitreoretinal disease and cataracts with pre-existing corneal astigmatism.

[*Ophthalmic Surg Lasers Imaging Retina.* **2013;44:XX-XX.**]

INTRODUCTION

Recent advanced sutureless vitrectomy techniques have hastened visual recovery, with reduction in postoperative astigmatism, conjunctival injection, pain, and discomfort.[1-7] The correction of refractive errors, including corneal astigmatism, has thus become a consideration in vitrectomy combined with cataract surgery. Toric intraocular lenses (IOLs) have been implanted in patients worldwide, and their feasibility has been demonstrated.[8-10] Over 30% of eyes indicated for cataract surgery have corneal astigmatism of at least 1.00 diopter (D).[11] Nevertheless, because of the technical difficulty of vitreous surgery and the emphasis on retinal disease control, toric IOLs have not been combined with vitrectomy surgery.

Twenty-five-gauge microincision vitrectomy surgery (25G MIVS) was first reported in 2002, and this technique is commonly used throughout the world.[12,13] Some patients (fewer than 1%) should forego MIVS or only undergo it with caution;[14] however, the indications for 25G MIVS have expanded to diseases including proliferative diabetic retinopathy (PDR), rhegmatogenous retinal detachment, giant retinal tear, intraocular foreign body, and IOL dislocation.[15-25] The increase in popularity of 25G MIVS has been enhanced by studies that have demonstrated its advantages for postoperative quality of vision. This is because intraoperative suturing is not required.[1-7] Recently, to prevent postoperative posterior capsule opacification (PCO) in patients with vitreoretinal disease who must have a vitrectomy combined with cataract surgery, a primary posterior capsulotomy technique using a 25-gauge vitreous cutter has been

From the Department of Ophthalmology, Tohoku University Graduate School of Medicine, Sendai, Japan (HK, NA, YM, TN); and the Division of Clinical Cell Therapy, Tohoku University Graduate School of Medicine, Sendai, Japan (TA).

Presented at the Sendai Toric IOL Conference, November 3, 2011.

The authors have no financial or proprietary interest in the materials presented herein.

Address correspondence to Hiroshi Kunikata, MD, Department of Ophthalmology, Tohoku University Graduate School of Medicine, 1-1 Seiryo-machi, Aoba-ku, Sendai 980-8574, Japan; +81 22 717 7294, Fax: +81 22 717 7298; Email: kunikata@oph.med.tohoku.ac.jp.

doi:

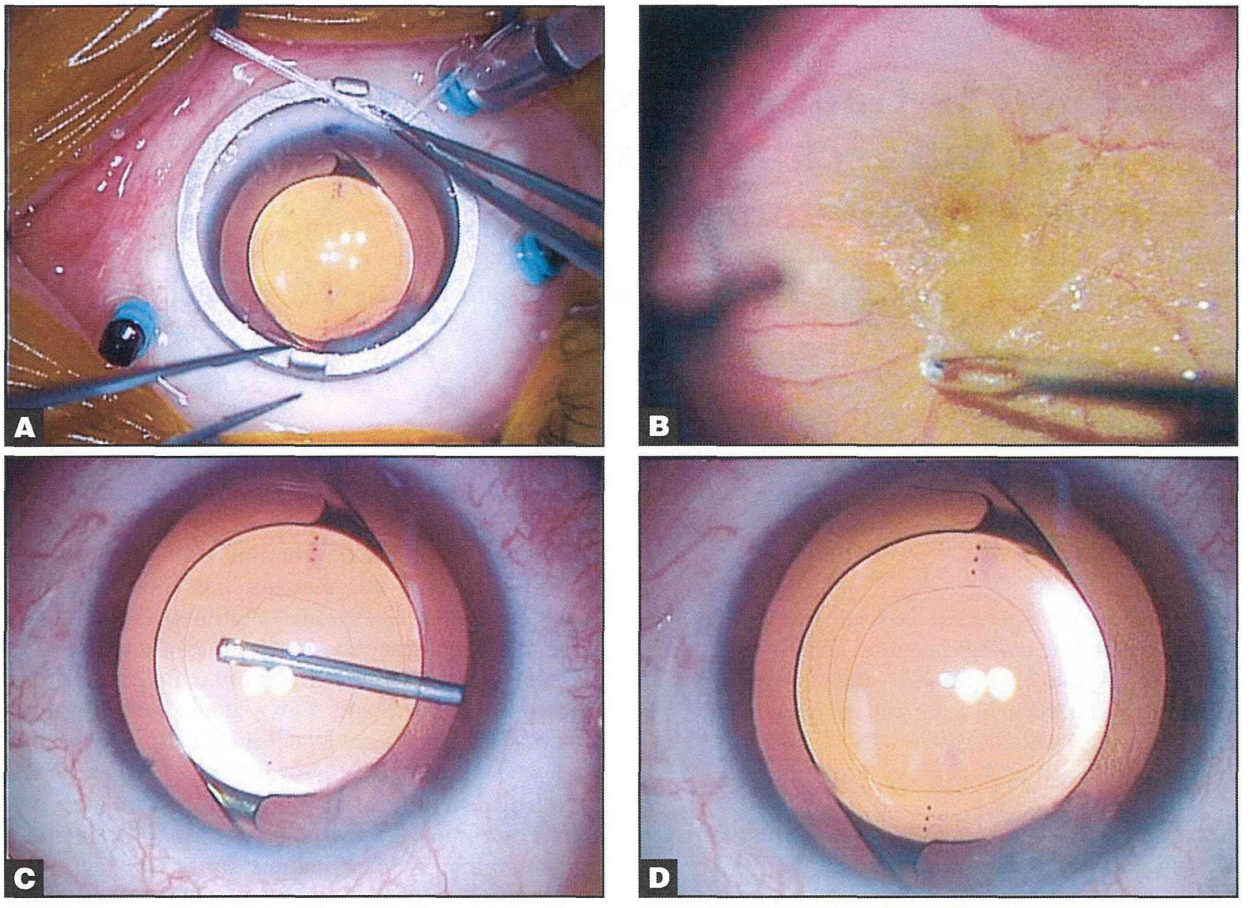

Figure 1. Representative eye with an epiretinal membrane (ERM) (Patient 2 in Table 1). Fundus and intraoperative photographs of the eye of a 60-year-old woman with an ERM. The eye had undergone combined 25-gauge microincision vitrectomy surgery (25G MIVS) and toric IOL implantation with posterior capsulotomy. (A) Intraoperative photograph of the anterior segment indicating a toric IOL implanted before 25G MIVS. (B) Intraoperative photograph of the fundus showing peeling of the epiretinal membrane, which was clearly visible thorough a toric IOL. (C) Intraoperative photograph of the anterior segment showing the center of the posterior capsule removed using a 25-gauge vitreous cutter. (D) The posterior capsule has been removed circularly and completely.

reported.[26,27] However, to the best of our knowledge, a procedure combining 25G MIVS and toric IOL implantation with posterior capsulotomy has not previously been reported, despite the large number of patients with concomitant vitreoretinal disease, cataracts, and pre-existing regular corneal astigmatism.

This report describes a technique combining 25G MIVS and toric IOL implantation with posterior capsulotomy.

PATIENTS AND METHODS

We reviewed the medical records of six consecutive eyes with retinal disease, cataracts, and corneal astigmatism that had undergone a combined surgery of phacoemulsification, toric IOL implantation with posterior capsulotomy, and 25G MIVS. The retinal diseases included epiretinal membrane (ERM) (eight eyes), macular hole (MH) (three eyes), and PDR (one eye). Preoperative demographics and surgical outcomes are shown in Table 1. Only eyes that had undergone a combined surgery of phacoemulsification, toric IOL implantation with posterior capsulotomy, and 25G MIVS by a single surgeon (HK) at the Surgical Retina Service at Tohoku University Hospital in Sendai, Japan, from February 2011 through March 2012 were included. Eyes with no corneal astigmatism, zonular weakness, or history of 23-gauge MIVS were excluded.

After explanation of the procedure, its purpose, risks and benefits, informed consent was obtained. The study conformed to the tenets of the Declaration of Helsinki and was approved by the institutional review board of the Tohoku University School of Medicine.

PREOPERATIVE ASSESSMENT AND INTRAOCULAR LENS

All patients were examined by slit lamp with pupils completely dilated. Axial length was measured

TABLE 1

Patient Demographics and Visual Improvement After Implantation of the Toric IOL and Axis Rotation of the Toric IOL Between Follow-up Visits in 12 Eyes

Patient No.	Age (Y)	Sex	Diagnosis	Preop Absolute Corneal Cylinder (D)	Postop Absolute Refractive Cylinder (D)	Visual Acuity (logMAR)				Intraop F/G Exchange	Axis of Toric IOL (Degrees)				
						UCVA		BCVA			Intended	1 Week Postop	1 Mos Postop	6 Mos Postop	Final Rotation
						Preop	Postop	Preop	Postop						
1	62	F	ERM	2.00	1.00	1.40	0.05	0.00	−0.08	N	101	91	93	95	6
2	60	F	ERM	2.00	0.25	1.15	0.00	0.05	−0.08	N	83	74	71	74	9
3	61	M	ERM	2.25	2.00	1.40	1.22	0.10	−0.08	N	86	89	87	89	3
4	70	F	ERM	1.50	0.25	0.22	0.05	0.22	−0.18	N	179	166	166	167	12
5	63	F	ERM	2.50	1.00	1.00	0.40	−0.08	0.30	N	96	93	91	92	4
6	53	M	ERM	1.50	0.50	1.05	0.05	0.00	−0.08	N	88	95	96	95	7
7	77	F	ERM	1.50	1.50	1.00	0.00	0.30	0.00	N	18	26	28	21	3
8	64	F	ERM	1.50	0.50	1.52	1.00	0.30	0.10	N	84	86	89	86	2
9	68	M	MH	2.75	0.75	0.70	0.52	0.70	0.10	Y	169	166	171	175	6
10	63	F	MH	2.00	0.75	0.70	−0.08	0.70	−0.08	Y	93	84	85	84	9
11	66	F	MH	1.25	0.75	0.82	0.40	0.70	−0.08	Y	53	52	51	50	3
12	66	F	PDR	1.75	0.25	1.40	−0.08	1.15	−0.08	N	169	168	166	173	4
Mean	64.4			1.88	0.79	1.03	0.29	0.34	−0.02						5.7

Preoperative corneal cylinder versus postoperative refractive cylinder, Wilcoxon signed-rank test: P = .003. Preoperative UCVA versus postoperative UCVA, Wilcoxon signed-rank test: P = .002. Preoperative BCVA versus postoperative BCVA, Wilcoxon signed-rank test: P = .015.

IOL = intraocular lens; UCVA = uncorrected visual acuity; BCVA = best corrected visual acuity; logMAR = logarithm of the minimum angle of resolution; F/G = fluid-air; ERM = epiretinal membrane; MH = macular hole; PDR = proliferative diabetic retinopathy.

using A-scan biometry (UD-7000; Tomey, Nagoya, Japan). Corneal astigmatism was determined by manual keratometry (TONOREF RKT-7700; Nidek, Aichi, Japan). The target postoperative spherical equivalent was aimed at emmetropia or –0.5 using the SRK/2 formula. IOL cylinder power and alignment axis were calculated using a Web-based toric IOL calculator program (http://www.acrysoftoriccalculator.com). This was done in patients with pre-existing regular corneal astigmatism greater than 1 D, taking into account the keratometry readings and mandatory data input on the position of the incision and surgery-induced astigmatism at an 11 o'clock corneal incision (0.50 D). The toric IOL design was based on the one-piece AcrySof platform (Alcon Laboratories, Fort Worth, TX). The overall haptic length was 13.0 mm, and the optic diameter was 6.0 mm. Three IOL variations (AcrySof SN6AT3, SN6AT4, and SN6AT5) treat different levels of pre-existing corneal astigmatism.

Corneal, internal, and ocular aberration were assessed preoperatively and 1 week, 1 month, and 6 months postoperatively with a wavefront analyzer (KR-9000PW; Topcon, Tokyo, Japan).

With the patient seated and under slit lamp to avoid ocular torsion, the 6 o'clock position was marked at the corneal limbus using a 27-gauge needle.

SURGICAL PROCEDURE

Under retrobulbar anesthesia, first the actual implantation axis was marked using a two-blade DK axis marker 9-729 and Mendez degree gauge 9-707R-1 (both Duckworth & Kent, Hertfordshire, England). Then three ports for 25G MIVS were created using the oblique sclerotomy technique with the Accurus vitrectomy system (Alcon Laboratories, Fort Worth, TX).[28] An infusion cannula was inserted through the inferotemporal sclera, followed by the insertion of two cannulas through the superotemporal and the superonasal regions.

A 2.4-mm corneal incision at the 11 o'clock position, continuous curvilinear capsulorrhexis, phacoemulsification using the divide-and-conquer technique, and irrigation/aspiration were performed. The toric IOL was implanted into the capsular bag with a Monarch 3 injector (Alcon Laboratories, Fort Worth, TX) and a D cartridge. Subsequently, the IOL was rotated with a lens hook so that the cylindrical axis of the lens was aligned with the corneal marks of the corneal astigmatism. Then viscosurgical material was removed gently by irrigation/aspiration.

After completion of IOL implantation, a sutureless contact lens was placed on the cornea to view the vitreal cavity. 25G MIVS was performed, comprising core vitrectomy, creation of a posterior vitreal detachment, peripheral vitrectomy, and ERM and internal limiting membrane (ILM) peeling. Endolaser photocoagulation was performed for the case with PDR. Fluid/air exchange was performed in the eyes with MH. Finally, just after the procedure was complete, the axis alignment of the implanted toric IOL was rechecked.

Antibiotics and corticosteroids were injected subconjunctivally at the end of surgery in all cases. All patients were prescribed a combination of antibiotic and corticosteroid eye drops four times daily and nonsteroid anti-inflammatory eye drops two times daily for 4 weeks.

POSTOPERATIVE MEASUREMENTS

One month postoperatively, uncorrected visual acuity (UCVA), best corrected visual acuity (BCVA), subjective refraction, and slit lamp examination were recorded, and postoperative corneal astigmatism was assessed by A-scan biometry. When the axis of the toric lens was measured, the pupil was dilated to enable visualization of the three dots on the optic periphery. The anterior segment was imaged with slit photography. A black measurement line and a circular scale in the periphery with single degree steps were then overlaid on the photograph so that the angle could be read. The axis of the toric IOL was evaluated at 1 week, 1 month, and 6 months postoperatively.

The patients were evaluated for intraoperative and postoperative complications associated with the surgery.

STATISTICAL ANALYSES

Data are presented as the mean ± standard deviation. The significance of the difference between the pre- and postoperative data was determined by Wilcoxon signed-rank tests or the Friedman test. The decimal BCVA was converted to logarithm of the minimal angle resolution (logMAR) units for statistical analysis. A P value of less than 0.05 was considered to be statistically significant.

RESULTS

As summarized in Table 1, there were three men and nine women, with a mean age at the time of surgery of 64.4 ± 5.9 years. All patients underwent 25-gauge MIVS and implantation of the toric IOL with posterior capsulotomy. All of the IOLs were successfully fixed in the capsular bag. The ERMs and ILMs were successfully removed in all eight eyes with ERM, and the ILMs were removed and fluid/air exchange was performed after insertion of the toric IOL in the three eyes with MH. The implanted toric IOL was stable during the fluid/air exchange procedure,

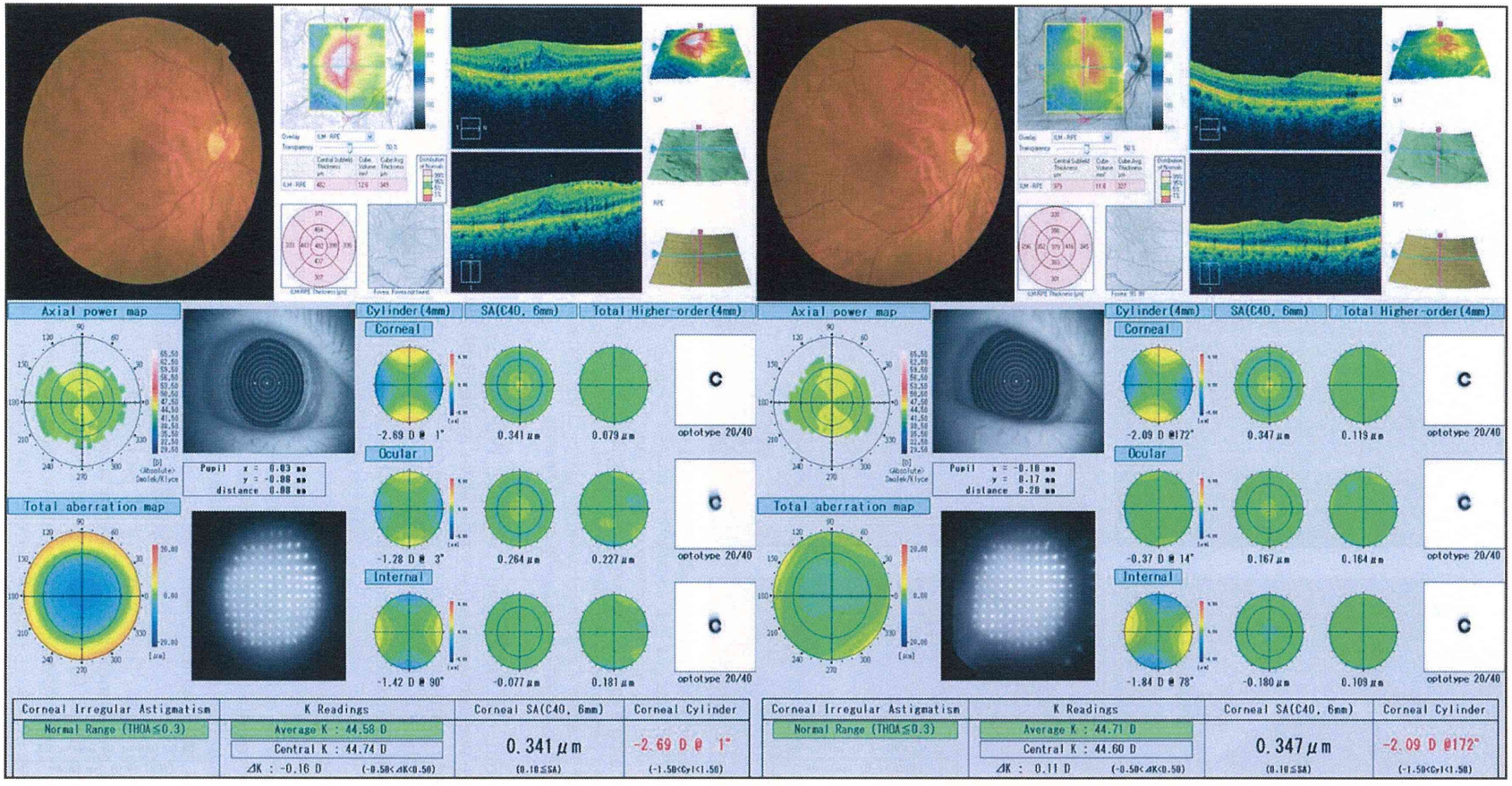

Figure 2. Representative eye (Patient 2 in Table 1) with an epiretinal membrane (ERM) (Patient 2; see Table 1). Preoperative and postoperative findings of the eye of a 60-year-old woman with an ERM. The eye had undergone combined 25-gauge micro incision vitrectomy surgery (25G MIVS) and toric IOL implantation with posterior capsulotomy. (Upper left) Preoperative photograph of the right fundus and findings of optical coherent tomography showing ERM and thickened foveal thickness, respectively. (Upper right) Postoperative photograph of the right fundus and findings of optical coherent tomography showing no ERM and decreased foveal thickness, respectively. (Lower left) Preoperative findings of a wavefront analyzer showing cylindrical with-the-rule corneal astigmatism. The ocular total cylindrical astigmatism was decreased slightly because the internal cylindrical astigmatism (cataract) corrected the corneal astigmatism slightly. Preoperatively, logMAR uncorrected visual acuity (UCVA) and best corrected visual acuity (BCVA) in this eye were 1.15 and 0.05, respectively. (Lower right) Postoperative findings of a wavefront analyzer showing cylindrical with-the-rule corneal astigmatism, unchanged from the preoperative condition. The ocular total cylindrical astigmatism was almost completely corrected postoperatively because the internal cylindrical astigmatism (toric IOL) had a strong corrective effect on the corneal astigmatism. Postoperatively, logMAR UCVA and BCVA in this eye were 0 and –0.08, respectively.

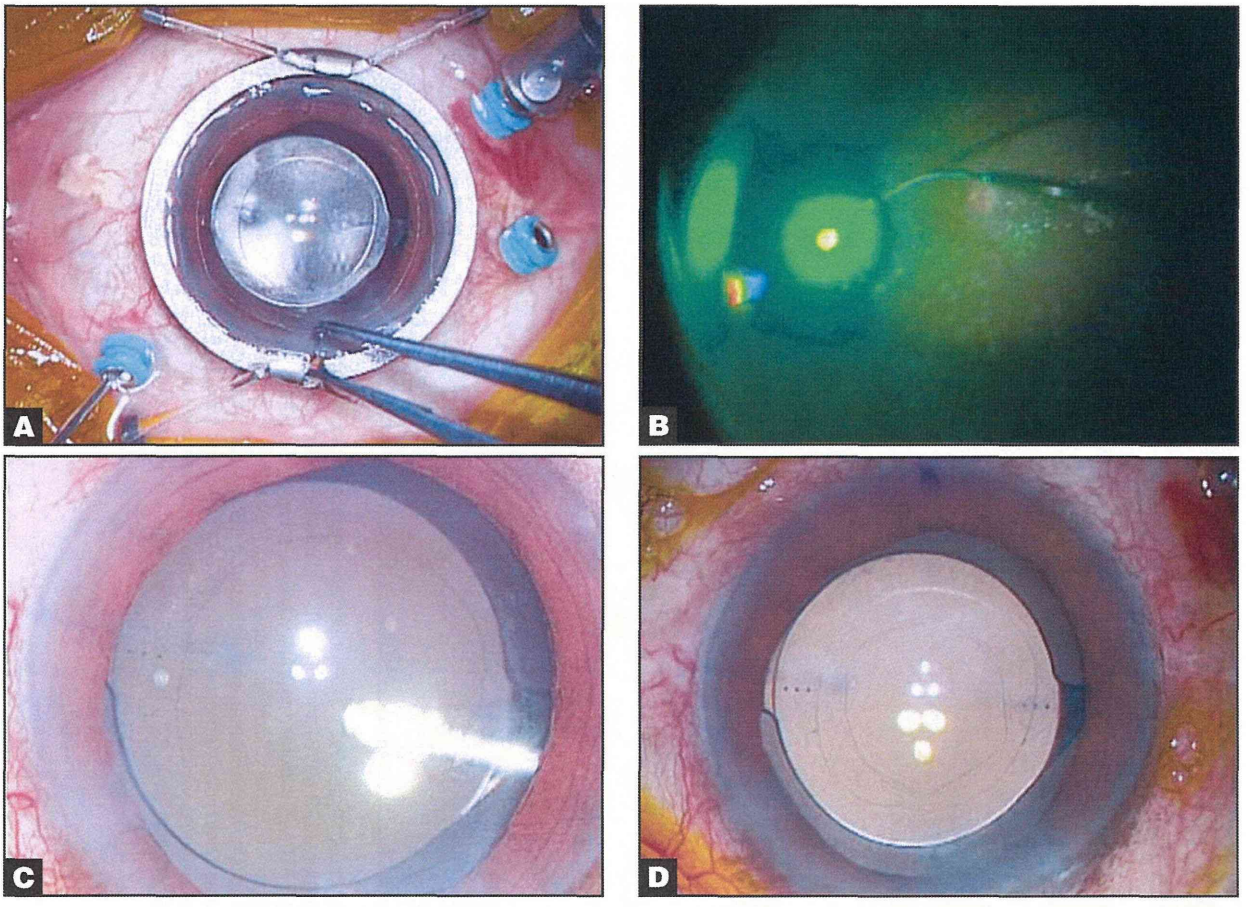

Figure 3. Representative eye with proliferative diabetic retinopathy (PDR) (Patient 12 in Table 1). Fundus and intraoperative photographs of the eye of a 66-year-old woman with PDR. The eye had undergone combined 25-gauge microincision vitrectomy surgery (25G MIVS) using the wide-viewing system and toric IOL implantation with posterior capsulotomy (posterior capsulotomy). (A) Intraoperative photograph of the anterior segment indicating a toric IOL implanted before 25G MIVS. (B) Intraoperative photograph of the fundus showing endolaser photocoagulation being performed to complete panretinal photocoagulation, which was clearly visible thorough a toric IOL. (C) Intraoperative photograph of the anterior segment showing the center of the posterior capsule removed using a 25-gauge vitreous cutter. (D) The posterior capsule has been removed circularly and completely.

and the MH was closed postoperatively. In the eye with PDR, the vitreous hemorrhage was removed successfully and endolaser performed complete panretinal photocoagulation. In all cases, the IOL was stably fixed and remained well-positioned at final examination.

The preoperative absolute corneal cylinder (mean cylinder) was 1.88 ± 0.46 D, and the 1-month postoperative absolute residual refractive cylinder was 0.79 ± 0.53 D. The postoperative residual refractive cylinder was significantly lower than the pre-existing regular corneal cylinder (P = .003, Wilcoxon signed-rank test).

UCVA and BCVA improved in all cases. The mean postoperative logMAR UCVA at 1 and 6 months was 0.31 ± 0.42 and 0.29 ± 0.43, respectively (P = 0.002, Wilcoxon signed-rank test), which was significantly better than the preoperative UCVA of 1.03 ± 0.38 (P = 0.002, Wilcoxon signed-rank test). The mean postoperative logMAR BCVA at 1 and 6 months was 0.05 ± 0.18 and –0.02 ± 0.13 (P = .023, Wilcoxon signed-rank test), respectively, which was significantly better than the preoperative BCVA of 0.34 ± 0.38 (P = .015, Wilcoxon signed-rank test). There was no difference between logMAR UCVA at 1 and 6 months (P = .69, Wilcoxon signed-rank test) or logMAR BCVA at 1 and 6 months (P = .35, Wilcoxon signed-rank test). The logMAR UCVA and BCVA improved to zero or less at 1 month in three of 12 patients (25%) and seven of 12 patients (58%), respectively. The logMAR UCVA and BCVA improved to 0 or less at 6 months in four of 12 patients (33%) and nine of 12 patients (75%), respectively.

In all cases, the IOL was stably fixed and remained well-positioned without a remarkable degree of rotation. The mean toric IOL axis rotation at 1 week, 1

month, and 6 months postoperatively was 5.8 ± 4.1°, 6.4 ± 4.0°, and 5.7 ± 3.1°, respectively, and the values were statistically similar at 1 week, 1 month, and 6 months ($P = .64$, Friedman test).

We did not suture the corneal wound or scleral ports in any of our cases. There were no intraoperative complications. In the eye with PDR, there was a temporary postoperative posterior iris synechia, but it released naturally, without any additional surgical intervention. No PCO, bacterial endophthalmitis, or other postoperative complications occurred.

Intraoperative findings in a representative case with ERM (Patient 2 in Table 1) are shown in Figure 1. Preoperative and postoperative findings in the same case (Patient 2 in Table 1) are shown in Figure 2. Intraoperative findings in a representative case with PDR (Patient 12 in Table 1) are shown in Figure 3. Preoperative and postoperative findings in the same case (Patient 12 in Table 1) are shown in Figure 4.

DISCUSSION

We set out to evaluate the efficacy of combined 25G MIVS and toric IOL implantation with posterior capsulotomy. Our study shows that this procedure is a practical and safe method for use in eyes with both vitreoretinal disease and corneal astigmatism. We observed a postoperative residual refractive cylinder significantly lower than the pre-existing regular corneal cylinder, as well as very rapid and sustained improvement of postoperative vision, with no occurrence of PCO. Axis rotation of the toric IOLs was minimal, and they were stably fixed 1 week postoperatively, and remained thus 6 months postoperatively.

Our study supports existing evidence that rapid visual improvement time makes 25G MIVS preferable to conventional 20-gauge pars plana vitrectomy (PPV) for the treatment of macular pucker or macular hole.[3,6] When 20-gauge PPV is used, suturing of the sclerotomy sites is required, and the sutures can induce postoperative astigmatism.[2,3,5-7] Our study also confirms existing data showing that acrylic toric IOLs are rotationally stable in the first 6 months postoperatively.[29,30] Furthermore, our study confirms existing data showing that 25G MIVS with posterior capsulotomy can prevent PCO.[26,27]

To achieve high-quality vision at an early postoperative stage in patients with retinal disease and corneal astigmatism, it is necessary to both correct the corneal astigmatism and thoroughly treat the retinal disease. The astigmatism of cataracts can offset corneal astigmatism (Figure 2), which then affects vision negatively after 25G MIVS and conventional (nontoric) IOL implantation. Currently, many patients over 50 years of age with retinal disease and cataract undergo a combination of 25G MIVS and IOL implantation, because if the cataract is left, it will progress after the operation. However, many such patients have regular corneal astigmatism and would benefit from use of a toric rather than conventional IOL. We believe that eyes with ERM, in particular, that start with high visual acuity should undergo combined 25G MIVS and toric IOL implantation if the eyes meet the criteria.

In our procedures, we simultaneously performed posterior capsulotomy. In posterior capsulotomy, the loss of the barrier between the anterior chamber and vitreous cavity raises concern about the possibility of postoperative endophthalmitis, but none occurred in our cases. We have reported that gas leaked from the vitreous cavity, through the posterior capsulotomy, and into the anterior chamber in cases in which fluid-air exchange was performed.[27] Thus, there was concern about the possibility of postoperative rotation of the toric IOL in our three cases with MH, because gas tamponade and a prone position can have negative effects on the implanted toric IOL. However, we saw no remarkable degree of rotation.

There are two advantages to combining 25G MIVS and toric IOL implantation with posterior capsulotomy. First, in patients with vitreoretinal disease requiring a vitrectomy combined with cataract surgery, a primary posterior capsulotomy technique using a 25-gauge vitreous cutter can prevent postoperative posterior capsule opacification,[26] thereby avoiding additional Nd:YAG laser treatment.[27] Secondly, posterior capsulotomy can release the fluid between the IOL and posterior capsule into the vitreous cavity, so that the posterior capsule can completely attach to the posterior surface of the IOL. This may prevent intraoperative and postoperative IOL rotation. Although fluid/air exchange was performed after the insertion of a toric IOL in cases with MH, the toric IOL was sufficiently stable, and there was no remarkable degree of axis rotation intraoperatively or postoperatively (Table 1, Patients 9 through 11). In our cases, the mean toric IOL axis rotation was statistically similar 1 week, 1 month, and 6 months postoperatively, and the mean rotation at 6 months was within 6°.

We did not have any visual difficulties in peeling ERMs and ILMs when the 25-gauge instruments were seen through the implanted toric IOL (Figure 1, upper right). We believe that during macular surgery for toric IOL-implanted eyes, vitreous surgeons should not experience any problems visualizing the macular lesion, because toric IOLs are made for the macula to focus on with less astigmatism. By contrast, if a peripheral lesion were seen through a floating contact lens and peripheral toric IOL, there could be prob-